Applied Physics Letters

Doping and compensation in heavily Mg doped Al-rich AlGaN films

Cite as: Appl. Phys. Lett. **120**, 082102 (2022); https://doi.org/10.1063/5.0082992
Submitted: 20 December 2021 • Accepted: 07 February 2022 • Published Online: 22 February 2022

Pegah Bagheri, Andrew Klump, Shun Washiyama, et al.

Applied Physics Letters ARTICLE scitation.org/journal/apl

Doping and compensation in heavily Mg doped Al-rich AlGaN films

Cite as: Appl. Phys. Lett. **120**, 082102 (2022); doi: 10.1063/5.0082992
Submitted: 20 December 2021 · Accepted: 7 February 2022 ·
Published Online: 22 February 2022

View Online Export Citation CrossMark

Pegah Bagheri,[1,a)] Andrew Klump,[1] Shun Washiyama,[1] M. Hayden Breckenridge,[1] Ji Hyun Kim,[1] Yan Guan,[1] Dolar Khachariya,[3] Cristyan Quiñones-García,[1] Biplab Sarkar,[1] Shashwat Rathkanthiwar,[1] Pramod Reddy,[2] Seiji Mita,[2] Ronny Kirste,[2] Ramón Collazo,[1] and Zlatko Sitar[1,2]

AFFILIATIONS

[1]Department of Materials Science and Engineering, North Carolina State University, Raleigh, North Carolina 27695-7919, USA
[2]Adroit Materials, Cary, North Carolina 27518, USA
[3]Department of Electrical and Computer Engineering, North Carolina State University, Raleigh, North Carolina 27695-7911, USA

[a)]Author to whom correspondence should be addressed: pbagher@ncsu.edu

ABSTRACT

Record low resistivities of 10 and 30 Ω cm and room-temperature free hole concentrations as high as 3×10^{18} cm^{-3} were achieved in bulk doping of Mg in $Al_{0.6}Ga_{0.4}N$ films grown on AlN single crystalline wafer and sapphire. The highly conductive films exhibited a low ionization energy of 50 meV and impurity band conduction. Both high Mg concentration ($>2 \times 10^{19}$ cm^{-3}) and low compensation were required to achieve impurity band conduction and high p-type conductivity. The formation of V_N-related compensators was actively suppressed by chemical potential control during the deposition process. This work overcomes previous limitations in p-type aluminum gallium nitride (p-AlGaN) and offers a technologically viable solution to high p-conductivity in AlGaN and AlN.

Aluminum gallium nitride (AlGaN) is used in deep-ultraviolet (UV) optoelectronic devices[1–3] as its emission wavelength can be tuned across the entire UV spectrum. This spectral range has many practical applications, such as sterilization, UV curing, biomedical instrumentation, and non-line of sight communication.[1,4] To date, many groups have demonstrated light-emitting diodes (LEDs) with emission wavelengths below 300 nm by using AlGaN, although with significantly lower external quantum efficiencies than achieved in their visible LED counterparts.[5–7] Similarly, optical pumping of AlGaN multiple-quantum-wells (MQWs) below 300 nm has produced lasing and very recently electrically injected 271 nm wavelength lasing.[8–10] However, significant improvements in the efficiency of these devices are required before they become competitive with current UV sources.

The poor conductivity of the p-type contact layer is one of the major challenges limiting AlGaN-based LEDs and laser diodes. This stems from the high ionization energy of the acceptors and the compensating point defects that are incorporated during the commonly used metalorganic chemical vapor deposition (MOCVD) growth.[11–13] The common dopant for realization of p-type conduction in GaN and AlGaN is Mg_{III}. Increasing the Al-content from GaN ($x = 0$) to AlN ($x = 1$) is expected to result in an increase in the ionization energy from 180 to 610 meV, respectively.[13,14] Consequently, only a small fraction of the total Mg generates holes at room temperature. Implementation of Be instead of Mg has been demonstrated recently to provide p-type conductivity in AlN with low ionization energy.[15] However, the transition of Be to interstitial sites and high concentrations of compensating point defects were found to limit p-type conductivity. Therefore, it is pivotal to understand the compensating donor-type point defects, which are energetically more favorable in p-type AlGaN and result in the poor electrical conduction.

Alternative approaches to bulk doping have been attempted to achieve a higher free carrier concentration (lower resistivity) for Al-rich AlGaN films. One approach utilized $Al_xGa_{1-x}N$/p-$Al_yGa_{1-y}N$ ($0 \leq x \leq 1, 0 \leq y \leq 1$) superlattice structures.[16,17] These structures generate a large sheet charge due to the polarization discontinuity at the heterojunction of different composition AlGaN alloys. Other approaches implemented the interface effect to efficiently reduce Mg activation energy and enhance the hole concentration in Al-rich AlGaN.[18] Another approach utilized films with graded Al-content AlGaN layers in which a three dimensional polarization induced charge is spread over the entire layer, increasing the hole concentration.[19] However, both superlattice and graded structures rely on a conducting p-GaN layer for p-contact formation. Since this layer will absorb any emission below 364 nm (the entire UV region), it

compromises the number of output photons from the active region. In short, obtaining a low resistivity p-AlGaN layer via bulk doping still plays a pivotal role for demonstration of high efficiency LEDs and laser diodes.

Work by Kinoshita *et al.* reopened the possibility for highly conductive bulk doping of AlGaN.[20] Interestingly, a relatively low ionization energy of ∼47–80 meV in p-$Al_{0.7}Ga_{0.3}N$ was reported for Mg doping of $\sim 10^{19}$ cm^{-3}, which likely invoked impurity band conduction, resulting in a resistivity of ∼47 Ω cm. Therefore, considering the high ionization energy of Mg in Al-rich AlGaN, heavy Mg doping is necessary to generate sufficient hole conduction at RT, making the impurity or native defect compensation the primary challenge. In addition, impurity band conduction can provide high hole concentration only via highly doping of Mg and reduction of compensating point defects. This can be addressed by systematic approaches developed for control of compensation, i.e., chemical potential control (CPC) and defect quasi Fermi level control (dQFLC).[21–23]

In this work, we present a study on high Mg doping in AlGaN coupled with the CPC scheme to control compensation during growth. This approach resulted in a record-low resistivity of 10 Ω cm in bulk Mg-doped $Al_{0.6}Ga_{0.4}N$.

Mg-doped $Al_{0.6}Ga_{0.4}N$ films were grown in a vertical, cold-walled MOCVD reactor at a pressure of 20 Torr on sapphire and AlN single crystal substrates. Growth on sapphire substrates was initiated with a 20 nm thick low temperature (650 °C) AlN nucleation layer, followed by a two-step 200 nm thick AlN template grown at 1120 and 1200 °C. These films were subjected to a 1700 °C anneal under flowing N_2 at atmospheric pressure for one hour to produce low dislocation density templates (LDD, $\sim 10^9$ cm^{-2}). The details on template formation are published elsewhere.[24] Finally, a 500 nm high temperature AlN layer followed by a 600 nm thick Mg doped $Al_{0.6}Ga_{0.4}N$ was grown on top of the LDD AlN template. All samples showed smooth surface with RMS roughness of <1 nm. In addition to growth on sapphire, Mg-doped $Al_{0.6}Ga_{0.4}N$ was grown also on an AlN single crystalline substrate (DD $< 10^4$ cm^{-2}) to assess the effect of dislocations on doping. The surface preparation and details on AlGaN epitaxial growth on AlN single crystals are described elsewhere.[25–27]

All Mg:AlGaN layers were grown at 1050 °C under H_2 diluent and 10 slm total flow. The growth rate was maintained constant at around 500 nm/h. Magnesium concentration ranging from 2×10^{19} to 1×10^{20} cm^{-3} was achieved by changing the flow rate of bis-(cyclopentadienyl) magnesium (Cp_2Mg) from 0.6 to 1.2 μmol/min. To control compensation, all films were grown at two different metal chemical potentials ∼1.9 and ∼2.0 eV [Ga process supersaturations of ∼13 (low) and ∼50 (high)], achieved by two different NH_3 flow rates, 0.3 (or V/III = 870) and 1 slm (or V/III = 2900), respectively. This change in the chemical potential decreased the probability for the formation of compensating defects by a factor of ∼3.

Quadrupole-SIMS (secondary ion mass spectroscopy) and time-of-flight (TOF) SIMS were used to quantify the concentrations of dopant (Mg) and various impurities (H, C, O, and Si) in as-grown and activation-annealed films. The activation-anneal was performed in an RTA (rapid thermal annealing) system at 850 °C, under flowing N_2 and for 20 min.

Temperature-dependent (200–800 K) electrical characterization was performed using an 8400 series LakeShore AC/DC Hall system. Standard Ni (20 nm)/Au (40 nm) contacts were deposited using e-beam evaporation and patterned for van der Pauw geometry, followed by contact annealing at 600 °C for 20 min in an air ambient. The dislocation density and Al content in AlGaN epilayers were estimated from x-ray diffraction (XRD) measurements using a Philips X'Pert materials research diffractometer with a Cu anode and using methods described elsewhere.[28]

To better understand Mg doping in AlGaN, it is useful to contrast it to Mg-doped GaN, which is well understood. Hydrogen in Mg:GaN plays a pivotal role in determining its resistivity.[29] During the MOCVD growth, it passivates Mg, forming the weakly bound Mg–H complex. This leads to resistivities greater than 1×10^6 Ω cm in as-grown Mg:GaN films. However, the formation of this complex is actually beneficial as it keeps the Fermi level close to the midgap and deprives the system of the driving force for making more irreversible changes, like formation of and complexing with vacancies. Following a post-growth thermal dissociation of the Mg–H complex and out-diffusion of hydrogen, the resistivity drops below 1 Ω cm.[23] The incorporation of hydrogen in GaN follows that of Mg one-to-one up to a concentration of $\sim 2 \times 10^{19}$ cm^{-3}, where it reaches its solubility limit.[30] Increasing the Mg concentration above 2×10^{19} cm^{-3} leads to self-compensation by nitrogen vacancies (V_N), which again increases the resistivity, but this time irreversibly.[23,29,31]

Figure 1 shows Mg and H concentrations in a Mg-doped $Al_{0.6}Ga_{0.4}N$ ladder structure grown under 1 slm of NH_3 and the same structure after the activation anneal. Although the H concentration increased with the increasing Mg concentration, in contrast to GaN, it stayed consistently significantly lower than [Mg]. In addition, and unlike in GaN, SIMS did not reveal a significant change in the H concentration after the activation anneal. This suggested that most of Mg in AlGaN was not passivated by H. It is important to note that C, O, and Si concentrations in all samples were constant throughout the ladder structure (not shown) at 8×10^{16}, 1.5×10^{17}, and 2×10^{16} cm^{-3}, respectively. Since they were orders of magnitude lower than [Mg], they were not considered to influence the electrical conduction. The "H limit" line corresponds to the maximum [H] observed in these samples and is similar to the one observed in GaN.[23]

Figure 2 shows resistivity, carrier concentration, and mobility in Mg-doped $Al_{0.6}Ga_{0.4}N$ for the two different NH_3 flow rates. At low ammonia flows of 0.3 slm (red data points in Fig. 2), the resistivity first decreased with the increase in [Mg] and then increased; samples with [Mg] $> 8 \times 10^{19}$ were too resistive for measurements on our hall system. The carrier concentration showed a maximum of $\sim 4 \times 10^{17}$ cm^{-3} at [Mg] $= 5 \times 10^{19}$ cm^{-3} and decreased with further increase in Mg concentration, as shown in Fig. 2(b). This "knee" behavior is characteristic for high doping in III-nitrides and indicates irreversible compensation by vacancy-related defect formation for both n- and p-dopants.[21] Formation of V_N-related complexes after the knee point were further verified by observation of defect luminescence at 3.8 eV with NBE emission at 5 ± 0.2 eV corresponding to $Al_{0.6}Ga_{0.4}N$ (not shown here).[32] Vacancy formation depends on the chemical potentials of species present during the growth, whereas the formation energy of V_N increases with the increasing N chemical potential, i.e., with the increasing ammonia flow, as established by Reddy *et al.*[22] Indeed, increasing the ammonia flow to 1 slm resulted in a decrease in resistivity and corresponding increases in carrier concentration and mobility, indicating a much lower compensation (black data points in Fig. 2). Although the characteristic knee behavior was not observed in this experimental set, it is expected to occur at some higher Mg doping level ($>10^{20}$ cm^{-3}). An increase in

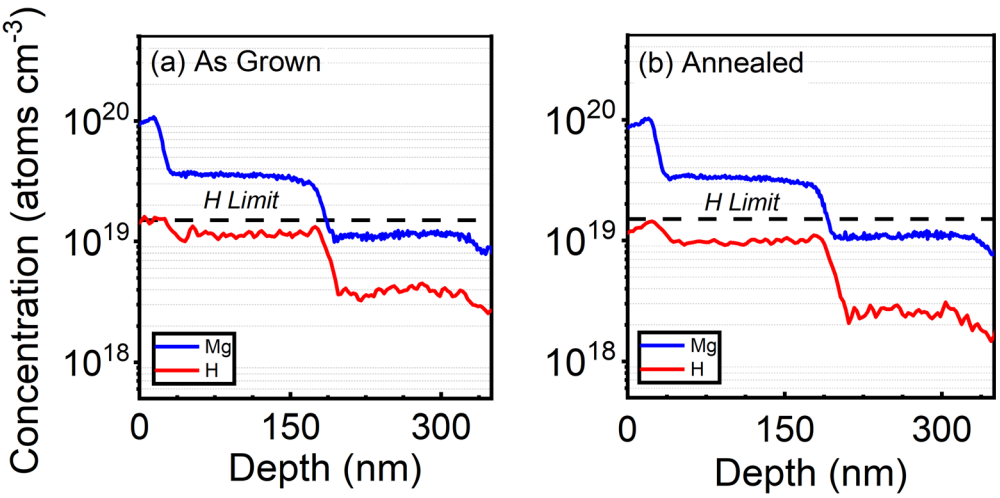

FIG. 1. SIMS of a Mg:$Al_{0.6}Ga_{0.4}N$ ladder structure grown under 1 slm of NH_3: (a) as grown and (b) after 850 °C activation anneal.

the NH_3 flow rate (or V/III) makes the growth environment richer in nitrogen and, therefore, increases the formation energy of V_N-related point defects.[11] Expectedly, suppression of V_N-related defects shifted the knee position in resistivity and carrier concentration from [Mg] $\sim 5 \times 10^{19}\,cm^{-3}$ to more than $10^{20}\,cm^{-3}$ where the heavy Mg doping became feasible. This heavy Mg doping and management of V_N compensation led to the lowest measured resistivity (30 Ω cm at $[Mg] = 10^{20}\,cm^{-3}$), which is the lowest value reported to date for high Al-content AlGaN grown on sapphire-based templates.

Interestingly, as seen in Fig. 2(b), black data points, the carrier concentration sharply increased for $[Mg] > 7 \times 10^{19}\,cm^{-3}$, which was associated with a sharp decrease in the mobility to $0.025\,cm^2/V\,s$ [Fig. 2(c)]. For high doping concentrations and low compensation, it is expected that an impurity band will form and the conduction will transition from valence-band-dominated to impurity-band-dominated transport.[33] As such, the results in Fig. 2 indicated that this transition occurred in lowly compensated Mg:AlGaN for $[Mg] > 7 \times 10^{19}\,cm^{-3}$.

It has been shown that dislocations have a profound influence on doping efficiency and electrical properties in wide bandgap semiconductors.[34] Since all of the above samples were grown on sapphire and had a dislocation density of $\sim 10^9\,cm^{-2}$, a Mg:$Al_{0.6}Ga_{0.4}N$ sample was grown on single crystal AlN with an average dislocation density of $< 10^4\,cm^{-2}$ for comparison. As seen in Fig. 2 (blue dots), under N-richer conditions, the removal of dislocations further reduced the resistivity by about one order of magnitude, as compared to similarly doped samples grown on sapphire. A resistivity of ~10 Ω cm and a free hole concentration of $3 \times 10^{18}\,cm^{-3}$ were measured for $[Mg] = 5 \times 10^{19}\,cm^{-3}$. Interestingly, the mobility does not seem to be affected much by the dislocation density reduction. It can be hypothesized that, for these high doping levels, the mobility is at first determined by ionized impurity scattering and eventually transitions into impurity band conduction.

To confirm the two conduction mechanisms, electrical properties of the Mg:AlGaN samples were studied as a function of temperature.

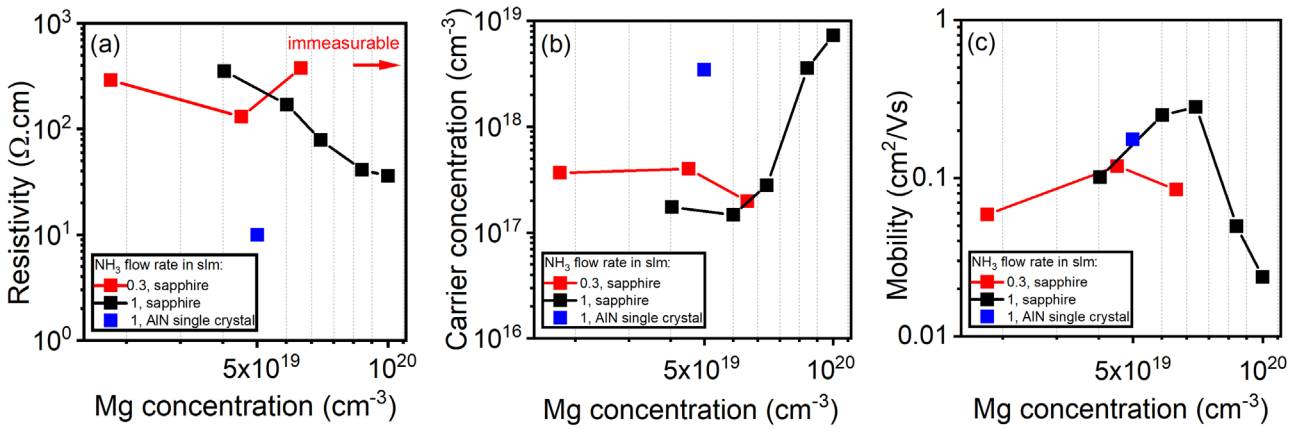

FIG. 2. Variation of (a) resistivity, (b) carrier concentration, and (c) mobility vs Mg concentration in $Al_{0.6}Ga_{0.4}N$ under 0.3 and 1 slm NH_3 flow rates on sapphire and AlN single crystal substrates. Solid lines were used as a guide to connect the data points.

Figure 3 shows the resistivity as a function of temperature for different Mg doping and compensation levels; the latter was achieved by changing the nitrogen chemical potential via NH_3 flow rate, as discussed above. All samples showed a two-slope behavior, indicative of two different carrier ionization energies. The low ionization energy at lower temperatures was attributed to the impurity band transport while a reduction in resistivity at higher temperatures suggested the onset of Mg ionization and, therefore, valence band transport.[20] Interestingly, by increasing Mg concentration, the transition from the impurity band to valence band transport occurred at higher temperatures. Comparing Figs. 3(a) (high compensation) and 3(b) (low compensation at similar Mg doping levels revealed that the transition from impurity band to the valence band occurred at a lower temperature under higher concentration of compensating point defects.

As shown in Fig. 4(a), a similar two-slope temperature dependence was observed for the sample grown on single crystalline AlN despite a significantly lower resistivity (10 Ω cm) attributed to low dislocation density. To extract the activation energies associated with each transport mechanisms, hole concentration vs temperature was considered [Fig. 4(b)]. The activation energy at low and high temperatures was estimated by using an Arrhenius dependence where the hole concentration is proportional to $\exp\left(\frac{-\Delta E_{impurity\_band}}{k_B T}\right)$ for impurity band transport and $\exp\left(\frac{-\Delta E_{Mg}}{2k_B T}\right)$ for valence band transport and negligible compensation, respectively.[35] The low ionization energy (~50 meV) at lower temperatures was attributed to the impurity band transport, while the higher slope at higher temperature (E_{Mg} ~ 360 meV) suggests the valence band transport. A similar behavior was observed previously for Mg doped $Al_{0.7}Ga_{0.3}N$, where the ionization energy was estimated to vary from ~50 to ~400 meV for low and high temperatures, respectively.[20] The mobility remained relatively constant at low temperatures, at about 0.3 cm^2/V s as shown in Fig. 4(c). This value is one order of magnitude lower than the expected mobility for the valence band transport. Thus, the observation of the low ionization energy and low mobility at low temperatures suggest that the dominant transport mechanism in highly p-doped $Al_{0.6}Ga_{0.4}N$ grown on AlN is also impurity band conduction. A sharp decrease in mobility is observed with raising temperature, mainly due to phonon and ionized Mg scattering.

From here, one can conclude that low Mg doping or high compensation ratio makes the impurity band formation less likely and, hence, valence band conduction dominates the transport in these samples, rendering samples highly resistive due to a high Mg ionization energy and high concentration of compensating point defects. On the other hand, the formation of the Mg impurity band requires both high doping and low compensation. It is important to note that the latter can be achieved only by targeted management of self-compensation (i.e., CPC method). Low activation energy for holes due to the impurity band provides two orders of magnitude higher hole concentration than the expected values for valence band transport in Mg doped $Al_{0.6}Ga_{0.4}N$ at this doping range. This offers a clear technological path to high hole concentrations and p-conductivity in AlGaN and AlN.

In conclusion, high Mg doping in $Al_{0.6}Ga_{0.4}N$ in the range of 2×10^{19}–1×10^{20} cm^{-3} was investigated. H incorporation did not follow that of Mg, suggesting that Mg in as-grown AlGaN was not passivated by H; a typical activation anneal as used in GaN did not result in any measurable changes in H concentration in AlGaN. Temperature dependent studies showed two ionization states of Mg: one at ~360 meV and one at ~50 meV, corresponding to valence band and impurity band conduction, respectively. The conductivity was found to be limited by the formation of V_N-related defects in both cases, thus managing these defects during growth was paramount to achieve high p-conductivity. The formation of the Mg impurity band required both high Mg doping concentration ($>2 \times 10^{19}$ cm^{-3}) and low compensation. By actively managing compensators during growth via chemical potential control, record low resistivities of 30 and 10 Ω cm were achieved for AlGaN grown on sapphire and AlN single crystalline wafers, respectively, with room temperature free hole concentrations

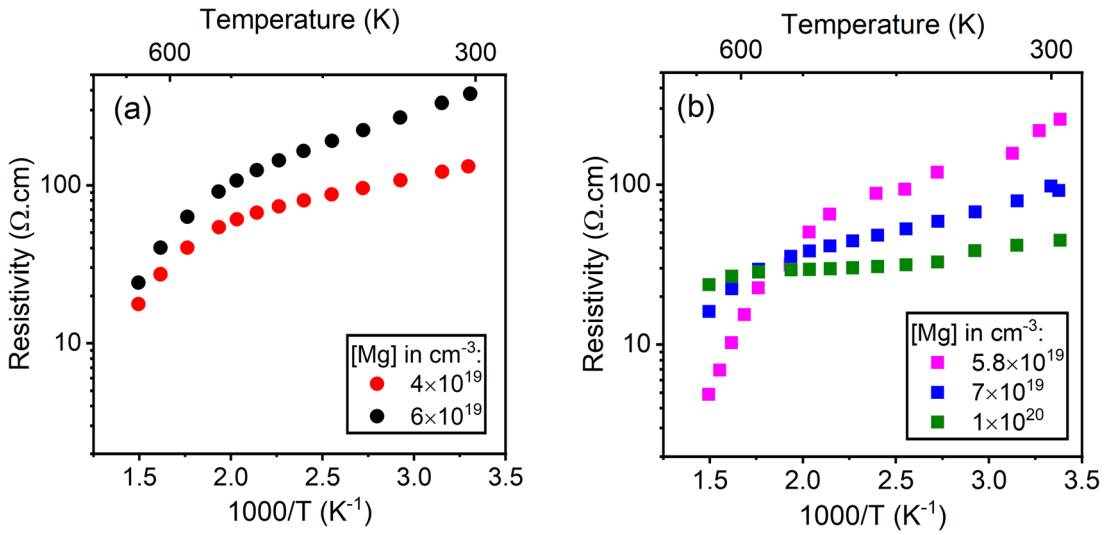

FIG. 3. Resistivity of Mg doped $Al_{0.6}Ga_{0.4}N$ grown on sapphire as a function of temperature: (a) 0.3 slm NH_3 flow, corresponding to V/III of 870; (b) 1 slm NH_3 flow corresponding to V/III of 2900. A change in slope indicates a transition between the valence band and impurity band transport.

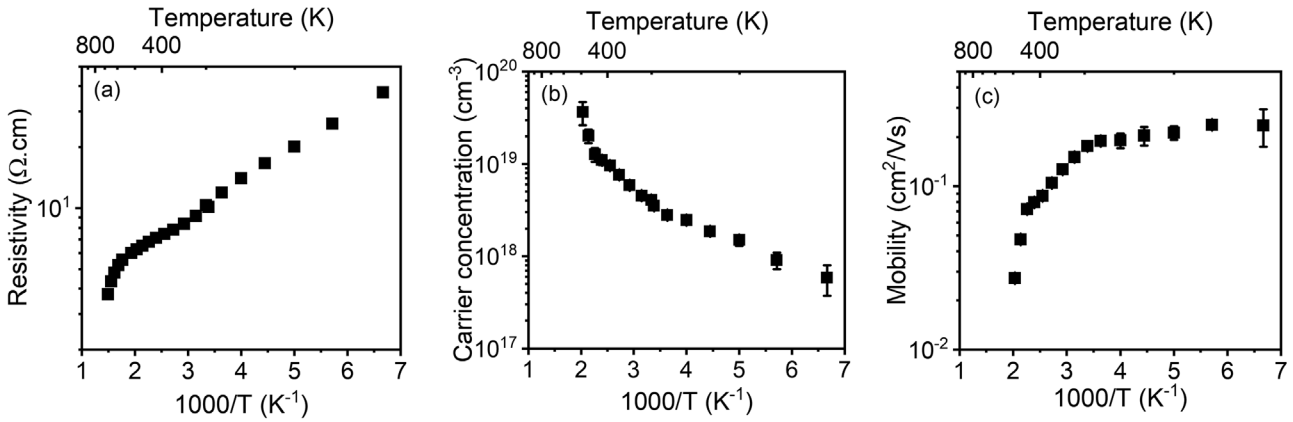

FIG. 4. (a) Resistivity, (b) carrier concentration, and (c) mobility as a function of temperature for $5 \times 10^{19}\,\mathrm{cm}^{-3}$ Mg doped $Al_{0.6}Ga_{0.4}N$ grown on an AlN single crustal substrate.

as high as $3 \times 10^{18}\,\mathrm{cm}^{-3}$. This approach lifts previous limitations in p-AlGaN and offers a viable technological path to high p-conductivity in high Al-content AlGaN and AlN.

The authors gratefully acknowledge funding in part from AFOSR (Nos. FA9550-17-1-0225, FA9550-19-1-0114, and FA9550-19-1-0358), NSF (Nos. ECCS-1508854, ECCS-1916800, and ECCS-1653383), and ARO (No. W911NF-16-C-0101).

AUTHOR DECLARATIONS

Conflict of Interest

The authors have no conflicts to disclose.

DATA AVAILABILITY

The data that support the findings of this study are available within the article.

REFERENCES

[1]J. Y. Tsao, S. Chowdhury, M. A. Hollis, D. Jena, N. M. Johnson, K. A. Jones, R. J. Kaplar, S. Rajan, C. G. V. de Walle, E. Bellotti, C. L. Chua, R. Collazo, M. E. Coltrin, J. A. Cooper, K. R. Evans, S. Graham, T. A. Grotjohn, E. R. Heller, M. Higashiwaki, M. S. Islam, P. W. Juodawlkis, M. A. Khan, A. D. Koehler, J. H. Leach, U. K. Mishra, R. J. Nemanich, R. C. N. Pilawa-Podgurski, J. B. Shealy, Z. Sitar, M. J. Tadjer, A. F. Witulski, M. Wraback, and J. A. Simmons, Adv. Electron. Mater. **4**, 1600501 (2018).
[2]H. Amano, R. Collazo, C. D. Santi, S. Einfeldt, M. Funato, J. Glaab, S. Hagedorn, A. Hirano, H. Hirayama, R. Ishii, Y. Kashima, Y. Kawakami, R. Kirste, M. Kneissl, R. Martin, F. Mehnke, M. Meneghini, A. Ougazzaden, P. J. Parbrook, S. Rajan, P. Reddy, F. Römer, J. Ruschel, B. Sarkar, F. Scholz, L. J. Schowalter, P. Shields, Z. Sitar, L. Sulmoni, T. Wang, T. Wernicke, M. Weyers, B. Witzigmann, Y.-R. Wu, T. Wunderer, and Y. Zhang, J. Phys. D: Appl. Phys. **53**, 503001 (2020).
[3]R. Kirste, B. Sarkar, P. Reddy, Q. Guo, R. Collazo, and Z. Sitar, J. Mater. Res. **36**, 4638 (2021).
[4]*III-Nitride Ultraviolet Emitters: Technology and Applications*, edited by M. Kneissl and J. Rass (Springer International Publishing, Cham, 2016).
[5]H. Hirayama, S. Fujikawa, N. Noguchi, J. Norimatsu, T. Takano, K. Tsubaki, and N. Kamata, Phys. Status Solidi A **206**, 1176 (2009).
[6]T. Nishida, H. Saito, and N. Kobayashi, Appl. Phys. Lett. **79**, 711 (2001).
[7]T. Nishida, T. Makimoto, H. Saito, and T. Ban, Appl. Phys. Lett. **84**, 1002 (2004).
[8]Z. Zhang, M. Kushimoto, T. Sakai, N. Sugiyama, L. J. Schowalter, C. Sasaoka, and H. Amano, Appl. Phys. Express **12**, 124003 (2019).
[9]Q. Guo, R. Kirste, S. Mita, J. Tweedie, P. Reddy, B. Moody, Y. Guan, S. Washiyama, A. Klump, Z. Sitar, and R. Collazo, J. Appl. Phys. **126**, 223101 (2019).
[10]H. Murotani, R. Tanabe, K. Hisanaga, A. Hamada, K. Beppu, N. Maeda, M. A. Khan, M. Jo, H. Hirayama, and Y. Yamada, Appl. Phys. Lett. **117**, 162106 (2020).
[11]C. Stampfl and C. G. Van de Walle, Appl. Phys. Lett. **72**, 459 (1998).
[12]C. G. Van de Walle and J. Neugebauer, J. Appl. Phys. **95**, 3851 (2004).
[13]J. L. Lyons, A. Janotti, and C. G. Van de Walle, Phys. Rev. Lett. **108**, 156403 (2012).
[14]J. Li, T. N. Oder, M. L. Nakarmi, J. Y. Lin, and H. X. Jiang, Appl. Phys. Lett. **80**, 1210 (2002).
[15]H. Ahmad, J. Lindemuth, Z. Engel, C. M. Matthews, T. M. McCrone, and W. A. Doolittle, Adv. Mater. **33**, 2104497 (2021).
[16]P. Kozodoy, Y. P. Smorchkova, M. Hansen, H. Xing, S. P. DenBaars, U. K. Mishra, A. W. Saxler, R. Perrin, and W. C. Mitchel, Appl. Phys. Lett. **75**, 2444 (1999).
[17]K. Ebata, J. Nishinaka, Y. Taniyasu, and K. Kumakura, Jpn. J. Appl. Phys., Part 1 **57**, 04FH09 (2018).
[18]X. Qiu and H. Jiang, Cryst. Growth Des. **21**, 2389 (2021).
[19]Z. Zhang, M. Kushimoto, M. Horita, N. Sugiyama, L. J. Schowalter, C. Sasaoka, and H. Amano, Appl. Phys. Lett. **117**, 152104 (2020).
[20]T. Kinoshita, T. Obata, H. Yanagi, and S. Inoue, Appl. Phys. Lett. **102**, 012105 (2013).
[21]S. Washiyama, P. Reddy, B. Sarkar, M. H. Breckenridge, Q. Guo, P. Bagheri, A. Klump, R. Kirste, J. Tweedie, S. Mita, Z. Sitar, and R. Collazo, J. Appl. Phys. **127**, 105702 (2020).
[22]P. Reddy, S. Washiyama, F. Kaess, R. Kirste, S. Mita, R. Collazo, and Z. Sitar, J. Appl. Phys. **122**, 245702 (2017).
[23]A. Klump, M. P. Hoffmann, F. Kaess, J. Tweedie, P. Reddy, R. Kirste, Z. Sitar, and R. Collazo, J. Appl. Phys. **127**, 045702 (2020).
[24]S. Washiyama, Y. Guan, S. Mita, R. Collazo, and Z. Sitar, J. Appl. Phys. **127**, 115301 (2020).
[25]A. Rice, R. Collazo, J. Tweedie, R. Dalmau, S. Mita, J. Xie, and Z. Sitar, J. Appl. Phys. **108**, 043510 (2010).
[26]R. Dalmau, B. Moody, R. Schlesser, S. Mita, J. Xie, M. Feneberg, B. Neuschl, K. Thonke, R. Collazo, A. Rice, J. Tweedie, and Z. Sitar, J. Electrochem. Soc. **158**, H530 (2011).
[27]I. Bryan, A. Rice, L. Hussey, Z. Bryan, M. Bobea, S. Mita, J. Xie, R. Kirste, R. Collazo, and Z. Sitar, Appl. Phys. Lett. **102**, 061602 (2013).
[28]J. Tweedie, R. Collazo, A. Rice, J. Xie, S. Mita, R. Dalmau, and Z. Sitar, J. Appl. Phys. **108**, 043526 (2010).
[29]S. Nakamura, T. Mukai, M. S. M. Senoh, and N. I. N. Iwasa, Jpn. J. Appl. Phys., Part 2 **31**, L139 (1992).
[30]M. P. Hoffmann, J. Tweedie, R. Kirste, Z. Bryan, I. Bryan, M. Gerhold, Z. Sitar, and R. Collazo, in *Gallium Nitride Mater. Devices IX* (International Society for Optics and Photonics, 2014), p. 89860T.

[31]W. Götz, N. M. Johnson, D. P. Bour, M. D. McCluskey, and E. E. Haller, Appl. Phys. Lett. **69**, 3725 (1996).
[32]M. L. Nakarmi, N. Nepal, J. Y. Lin, and H. X. Jiang, Appl. Phys. Lett. **94**, 091903 (2009).
[33]D. Lancefield and H. Eshghi, J. Phys.: Condens. Matter **13**, 8939 (2001).
[34]I. Bryan, Z. Bryan, S. Washiyama, P. Reddy, B. Gaddy, B. Sarkar, M. H. Breckenridge, Q. Guo, M. Bobea, J. Tweedie, S. Mita, D. Irving, R. Collazo, and Z. Sitar, Appl. Phys. Lett. **112**, 062102 (2018).
[35]K. Seeger, *Semiconductor Physics: An Introduction* (Springer Science & Business Media, 2013).